Magnetic field conditions upstream of Ganymede

Marissa F. Vogt[1,1], Fran Bagenal[2,2], and Scott J Bolton[3,3]

[1]Boston University
[2]University of Colorado Boulder
[3]Southwest Research Institute

January 20, 2023

Abstract

Jupiter's magnetic field is tilted by ˜10º; with respect to the planet's spin axis, and as a result the Jovian plasma sheet passes over the Galilean satellites at the jovigraphic equator twice per planetary rotation period. The plasma and magnetic field conditions near Ganymede's magnetosphere therefore change dramatically every ˜5 hours, creating a unique magnetosphere-magnetosphere interaction, and on longer time scales as evidenced by orbit-to-orbit variations. In this paper we summarize the typical magnetic field conditions and their variability near Ganymede's orbit as observed by the Galileo and Juno spacecraft. We fit Juno data from orbit 34, which included the spacecraft's close Ganymede flyby in June 2021, to a current sheet model and show that the magnetospheric conditions during orbit 34 were very close to the historical average. Our results allow us to infer the upstream conditions at the time of the Juno Ganymede flyby.

Magnetic field conditions upstream of Ganymede

Marissa F. Vogt[1], Fran Bagenal[2], and Scott J. Bolton[3]

[1] Center for Space Physics, Boston University, Boston, MA, USA

[2] Laboratory for Atmospheric and Space Physics, University of Colorado Boulder, Boulder, CO, USA

[3] Southwest Research Institute, San Antonio, TX, USA

Corresponding Author: Marissa Vogt, mvogt@bu.edu

Key points

- The magnetic field magnitude and direction upstream of Ganymede vary strongly with longitude
- Temporal variations in the magnetosphere also influence Ganymede's upstream field conditions
- Juno's Ganymede flyby occurred during typical magnetospheric conditions

Abstract

Jupiter's magnetic field is tilted by ~10º with respect to the planet's spin axis, and as a result the Jovian plasma sheet passes over the Galilean satellites at the jovigraphic equator twice per planetary rotation period. The plasma and magnetic field conditions near Ganymede's magnetosphere therefore change dramatically every ~5 hours, creating a unique magnetosphere-magnetosphere interaction, and on longer time scales as evidenced by orbit-to-orbit variations. In this paper we summarize the typical magnetic field conditions and their variability near Ganymede's orbit as observed by the Galileo and Juno spacecraft. We fit Juno data from orbit 34, which included the spacecraft's close Ganymede flyby in June 2021, to a current sheet model and show that the magnetospheric conditions during orbit 34 were very close to the historical average. Our results allow us to infer the upstream conditions at the time of the Juno Ganymede flyby.

Plain Language Summary

Ganymede is the only moon in the solar system with an intrinsic magnetic field. This field forms a bubble in space around the moon, called a magnetosphere, that is itself contained within Jupiter's magnetosphere. The magnetic field and plasma conditions within Ganymede's magnetosphere can be used to infer information about the satellite's atmosphere, ionosphere, and interior. It is therefore important to understand the interaction between Ganymede's magnetosphere and the Jovian environment in the same way that we study the effects of space weather on the Earth. Here we analyze Galileo magnetic field measurements from Jupiter's magnetosphere in the region near Ganymede's orbit to establish the typical magnetic field magnitude and direction. We discuss the average conditions as well as the nature of the variability that occurs due to dynamic processes occurring in Jupiter's magnetosphere. This information provides useful context for analyzing data from Juno's recent flyby of Ganymede, which we show occurred during typical magnetospheric conditions.

1. Introduction

Jupiter's moon Ganymede is the only satellite in the solar system to possess its own intrinsic magnetic field, which creates a small magnetosphere that is embedded in Jupiter's inner magnetosphere (Kivelson et al., 1996). Ganymede is therefore a fascinating target for studying moon-magnetosphere interactions. Data and models from the Galileo flybys of Io, Europa, Ganymede, and Callisto show that changes in the upstream conditions, including the satellite's location with respect to Jupiter's plasma sheet, can have a major influence on the moon-magnetosphere interaction and produce an inductive response that can be used to probe the moons' internal structure (e.g. Kivelson et al., 1999, 2002). The observed magnetic field from within Ganymede's magnetosphere contains contributions from Ganymede's internal magnetic field, currents within Ganymede's magnetosphere, any inductive magnetic field from a possible subsurface liquid ocean inside the moon, and the magnetic field of Jupiter's magnetosphere (Kivelson et al., 2002). Therefore, it is important to quantify the range of magnetic field and plasma conditions that may be expected upstream of the Galilean satellites and to predict those conditions at the time of close spacecraft encounters.

The goals of this paper are 1) to establish the range of likely magnetic field conditions upstream of Ganymede by analyzing the available Galileo and Juno magnetometer data, and 2) to examine the magnetic field conditions near Ganymede during Juno's orbit 34 prior to and following its close flyby of Ganymede on 7 June 2021. We first consider how the magnetic field magnitude and direction near Ganymede change over the ~10 hour planetary rotation period as the satellite's magnetic latitude oscillates due to Jupiter's ~10º dipole tilt. We then consider how the magnetic field conditions change on longer timescales such as the orbit-by-orbit current sheet variability that has been studied in both Galileo and Juno data (e.g. Russell et al., 2001; Vogt et al., 2017; Connerney et al., 2020). Both of these types of variability in the upstream conditions occur on timescales that are long compared to the ~minutes long timescale for plasma circulation in Ganymede's magnetosphere (e.g. Jia et al., 2009, 2010; Toth et al., 2016; Zhou et al., 2020) and it is likely that conditions are always favorable for magnetopause reconnection (Kaweeyanun et al., 2020). But even if the upstream field conditions have only a limited influence on activity in Ganymede's magnetosphere, they can still affect the interpretation of magnetic field measurements near Ganymede. In particular, the magnetic field observed near Ganymede includes the contributions of both Jupiter's magnetosphere field and the field produced by Ganymede (intrinsic and induced), so an accurate estimate of the upstream conditions is important to constraining the properties of Ganymede's internal magnetic field. In our study we focus on the upstream magnetic field conditions though the plasma conditions are also both temporally and spatially variable (e.g. Kivelson et al., 2022), which will affect the nature of the satellite-magnetosphere interaction (e.g. Bagenal and Dols, 2020).

This paper is organized as follows: section 2 reviews the availability of magnetic field measurements near Ganymede's orbit and the expected dependence on longitude. Section 3 summarizes the Galileo magnetic field measurements near Ganymede and their spatial (longitudinal and local time) and temporal variability. In section 4 we examine the magnetospheric conditions before and after Juno's orbit 34 Ganymede flyby, and we conclude with a summary in section 5.

2. Data availability and expected longitudinal dependence

Magnetic field measurements from Jupiter's magnetosphere are available from six spacecraft that flew through the system (Voyager 1, Voyager 2, Pioneer 10, Pioneer 11, Ulysses) and two orbiters (Galileo, 1996-2003; and Juno, 2016-present). Figure 1 shows the orbital coverage of all spacecraft that have visited the Jovian system except Cassini, which only briefly entered Jupiter's magnetosphere, and New Horizons, which did not carry a magnetometer. The spacecraft trajectories are shown in magnetospheric local time, System III latitude and longitude, and magnetic coordinates ("wiggle plot") as calculated using the JRM09 dipole tilt value of 10.31º toward 196.61º System III left-handed longitude (Connerney et al., 2018). Galileo's orbit was confined to near the jovigraphic equatorial plane while Juno is in a polar 53-day orbit with an apoapsis of ~110 R_J and an inclination that is increasing with time (Bolton et al., 2017). During the inbound portion of its initial orbits Juno's latitude at ~10-20 R_J was as large as ~20º but that latitude has decreased with time.

Ganymede orbits Jupiter in a nearly circular path (eccentricity = 0.001) with a semi-major axis 14.97 R_J (1 R_J = 71,492 km) and an orbital inclination of 0.18º. For simplicity, in our analysis we will take "Ganymede's orbit" to mean a circular path of radius 15 R_J in Jupiter's jovigraphic equatorial plane. Most of the magnetic field measurements from the region near Ganymede's orbit come from Galileo, which completed over 30 orbits of Jupiter and collected magnetic field measurements with a typical time resolution of 24 seconds per vector. In just under half of its first 34 orbits, Juno passed through magnetic latitudes equivalent to the region near Ganymede's orbit, as shown in the bottom middle panel of Figure 1, though the spacecraft was typically located ~1 R_J or more off the jovigraphic equator (see top right panel of Figure 1). Juno magnetic field measurements are available with a time resolution of 1 second per vector (Connerney et al., 2017). The other spacecraft that passed Ganymede's orbit (Pioneer 10, Pioneer 11, Voyager 1, Voyager 2, Ulysses) were typically located significantly off the jovigraphic equator, so we exclude them from our statistical analysis in the next section.

The magnetic field in Jupiter's innermost magnetosphere (R < 10 R_J) is largely dipolar, while in the middle magnetosphere (R > 30 R_J) the field becomes radially stretched by the currents flowing in the current sheet or plasma sheet. Outside of the Io plasma torus, the plasma in Jupiter's magnetosphere is concentrated in a plasma sheet that is roughly aligned with the magnetic equator inside of ~30 R_J (Behannon et al., 1981). At Ganymede's orbit the magnetic equator and centrifugal equator, the point along each flux tube farthest from the planet, are nearly, but not exactly, aligned (Phipps and Bagenal, 2021). Jupiter's dipole field is tilted ~10º with respect to the planet's spin axis, toward ~200º west (left-handed) System III longitude. As a result, a spacecraft or moon near the jovigraphic equator – like Galileo and Ganymede – will observe the magnetic field fluctuating as its magnetic latitude oscillates from roughly +10º to -10º over the planet's ~10 hour rotation period. Therefore, both the magnitude and direction of the magnetic field upstream of Ganymede are strongly dependent on longitude. For example, the radial component of the magnetic field, B_R, reverses twice per planetary rotation as Jupiter's plasma sheet passes over the jovigraphic equator.

Figure 2, which we discuss further in the next section, shows the modeled longitudinal dependence of the magnetic field at Ganymede's orbit along with Galileo measurements from radial distances 14.95-15.05 R_J. A similar plot showing the longitudinal dependence of the magnetic field near Ganymede's orbit as measured during Juno's first 33 orbits is given in Figure 3; we exclude Juno data from Figure 2 because most orbits are significantly off the jovigraphic equator and therefore are not representative of the magnetic field conditions near Ganymede. The model field, shown by the thick gray lines, is calculated using the JRM09 model for Jupiter's internal field plus the contribution of a current sheet from the Connerney et al. (2020) model ("CON2020") at a radial distance of 15 R_J at the jovigraphic equator. This current sheet model is based on a Voyager-era model which represented Jupiter's current sheet as an axisymmetric washer-shaped disk (Connerney et al., 1981). The Voyager-era model fit parameters are the inner and outer edge of the disk, the disk thickness, the current sheet azimuthal tilt, the azimuthal angle of the tilt, and the azimuthal current constant $\frac{\mu_0 I_0}{2}$, which represents the current sheet current density and is given in units of nT. The CON2020 model updated the original Voyager-era model by introducing a radial current constant I_{rad}, in units of MA, that produces a B_φ, the azimuthal component of the magnetic field, and controls the field bend back out of the meridian plane. Fitting the current constants to Galileo and Juno data on an orbit-by-orbit basis has provided a measurement of temporal activity in Jupiter's magnetosphere and can give insights into the expected field variability at Ganymede's orbit (Vogt et al., 2017; Connerney et al., 2020). Finally, we note that other external field models (e.g. Khurana, 1997) predict similar magnetic field conditions near Ganymede's orbit, as shown in Figure S1.

3. Galileo magnetic field observations near Ganymede: spatial and temporal variability

The measurements and model predictions plotted in Figure 2 provide an overview of the typical magnetic field conditions upstream of Ganymede and their spatial and temporal variability. The figure shows the three field components in System III spherical coordinates, the magnetic field bendback and elevation angles, and the field magnitude as a function of longitude. The magnetic field bendback angle α indicates the angle of the magnetic field out of a meridian plane and is defined by $\alpha = \tan^{-1}\left(\frac{B_\varphi}{B_R}\right)$ so that a negative (positive) bendback angle indicates a swept back (swept forward) field configuration. The field elevation angle, $\theta_{elevation}$, indicates the angle that the magnetic field makes with respect to the radial direction in the R-θ plane and is defined by $\theta_{elevation} = \tan^{-1}\left(\frac{-B_\theta}{|B_R|}\right)$ so that the elevation angle is positive for a southward field and is 90º when the field is completely southward. We evaluate both angles only when $|B_R| > 3$ nT because small fluctuations in B_R can lead to large fluctuations in the field angles when B_R is small. The data plotted in Figure 2 are clustered in groups that each come from individual orbit inbound or outbound segments, with color indicating the spacecraft local time. Figure 2 includes all Galileo measurements at radial distances 14.95-15.05 R_J excepting the six close flybys of Ganymede when the spacecraft was measuring Ganymede's magnetospheric field. For the intervals plotted in Figure 2, the Galileo spacecraft was located at jovigraphic latitudes -1.57º to 3.27º.

The data and model predictions in Figure 2 show overall good agreement and can be used together to characterize the magnetic field conditions near Ganymede's orbit, which we summarize in Table 1. The measurements listed in Table 1 describe the range of field values measured by Galileo, excluding the close flyby encounters, at radial distances 14.95-15.05 R_J. The average $|B|$ value near Ganymede is ~95-100 nT according to both the data and model, and the field is typically oriented mostly in the north-south direction and only weakly swept out of the meridian plane (the model predicts $|B_\theta| > |B_R|$ and $|\alpha| < 20°$ at roughly 70 percent of longitudes). The magnetic field orientation is therefore generally favorable for reconnection at Ganymede's magnetopause since the satellite's internal magnetic field is oriented almost completely northward, with a dipole tilt of 176º from its spin axis (Kivelson et al., 2002; Kaweeyanun et al., 2020).

The field near Ganymede's orbit changes on time scales that are longer than the ~10 hour planetary rotation period, as shown by orbit-to-orbit changes in the observed field values plotted in Figure 2. Some of the orbit-to-orbit variation may be accounted for by the orbits' spatial, not temporal, differences. For example, the magnetic field and plasma properties in Jupiter's magnetosphere vary with local time (e.g. Palmaerts et al., 2017 and references therein), which means that the upstream magnetic field conditions change over the satellite's ~7 day orbital period. The local time dependence of the magnetic field is most evident in the meridional component, B_θ, which varies by ~9 nT (~10%) near Ganymede's orbit. Galileo measurements of the B_θ local time dependence near Ganymede are plotted in Figure S2, which shows that the data are reasonably well-fit by the longitudinally-averaged JRM09+CON2020 model plus the external B_θ local time fit of Vogt et al. (2017). The B_θ local time dependence can also be seen in Figure 2, as B_θ measurements collected at local times near 15:00 (purple and dark blue) are generally larger than those collected at local times far from 15:00 (green and red). We account for local time variations in the functional fits described in Appendix A. However, most of the orbit-to-orbit variability in the magnetic field indicates variable magnetospheric conditions due to activity like magnetospheric injections, mass loading due to volcanic activity on Io, or even changes in the external solar wind conditions (e.g. Mauk et al., 1999; Louarn et al., 2014; Tao et al., 2005; Vogt et al., 2019).

In general, the magnitude of these orbit-by-orbit temporal changes is significantly smaller than the magnitude of the variations with longitude. For example, the two dashed gray lines in Figure 2 show the expected range of the JRM09 + CON2020 modeled field conditions. To calculate these maximum and minimum model values we used the range of best fit current constants fit to individual Juno orbits listed in Table 2 of Connerney et al. (2020). The average temporal change in $|B|$ expected from the current sheet variability is ~5 nT, but it can be as large as ~12 nT near the magnetic equator. The modeled differences in the individual field components, which we list in Table 1, typically represent a ~10-20 percent variability in the baseline values (note that the change in B_R and B_φ depends strongly on longitude). Figure S3 illustrates how changes in the CON2020 current constants affect the predicted individual field components near Ganymede's orbit. In general, changes to the radial current constant I_{rad} have only a very small effect on B_R and B_θ but can significantly influence B_φ, particularly at high magnetic latitudes (near the longitude of the dipole tilt and 180º away from it). Near the magnetic equator only B_θ is strongly dependent on the azimuthal current constant $\frac{\mu_0 I_0}{2}$.

Connerney et al. (2020) reported that the current sheet variability during Juno's first 24 orbits, as determined by orbit-to-orbit changes in best-fit current constants, was roughly comparable to the variability reported in Galileo data by Vogt et al. (2017). However, the Juno measurements plotted in Figure 3 show significantly greater orbit-to-orbit variability than do the Galileo data from Figure 2. It is therefore important to note that the Juno data were collected at a larger range of jovigraphic latitudes than the near-equatorial Galileo data. Data in Figure 3 are plotted in colors indicating the average jovigraphic latitude of the spacecraft during the interval plotted for each orbit. The thin colored lines in Figure 3 show the longitudinal dependence of the JRM09+CON2020 model field at different jovigraphic latitudes. At the highest latitudes shown (15º and 20º latitude, in light and dark blue, respectively) the model field differs significantly from the near-equatorial field (e.g. 0º and 5º latitude, plotted in red and yellow, respectively) in terms of its magnitude, direction, and longitudinal dependence. Therefore, it is important to consider the latitude at which the Juno data were measured and compare Juno data only to model predictions evaluated at similar latitudes (e.g. by comparing data to a model line of a similar color in Figure 3). Though the Juno magnetic field data in Figure 3 display greater overall variability than the near-equatorial Galileo data in Figure 2 we conclude that most of that variability is due to the large latitudinal range of Juno's orbits.

In Figure 4 we show the values of the magnetic field measured by Galileo in the general vicinity of Ganymede, organized by position in magnetic cylindrical coordinates. Each panel is divided into boxes spanning 0.05 R_J in ρ_{mag} (cylindrical radial distance) by 0.25 R_J in z_{mag}, with color indicating quantities like the average or standard deviation of the measured magnetic field in each box. This figure gives insight into the expected field variability at Ganymede's orbit on both short (~10 hour) and long (orbit-by-orbit) time scales. The average B_R is very well-organized by magnetic coordinates, indicating that the B_R near Ganymede is relatively constant on long time scales (weeks to months) but varies strongly as Ganymede's position in magnetic coordinates (pink curves in Figure 4) change over a planetary rotation period. By comparison, the plot of the average B_φ is extremely disorganized, indicating that it is highly variable on long time scales.

Figure 4 also shows that the long-term temporal variability of B_R and B_θ, as indicated by the standard deviation plots, is typically ~ a few nT, which is roughly consistent with the CON2020 modeled temporal variability. This can also be seen in Figure 2, where the magnitude of the scatter in B_R and B_θ at a given longitude is roughly consistent with the modeled current sheet variability (the difference between the two dashed gray lines) but the scatter in the measured B_φ is significantly larger than the temporal variability predicted by the CON2020 model. Analogous plots made using Juno data are provided in Figure S4, though we note that each colored box typically contains data from only one Juno orbit because of the limited data coverage at low jovigraphic latitudes. Therefore, the standard deviations plotted in Figure S4, are typically smaller for Juno than for Galileo because they indicate temporal variability on short (seconds or minutes) timescales rather than orbit-to-orbit variability.

Finally, in Appendix A we derive functional fits to the Galileo magnetic field measurements near Ganymede. Existing global field models, including the JRM09 + CON2020 model and the Khurana (1997) model, show good agreement with the data throughout the inner and middle magnetosphere. However, by focusing just on the data collected near Ganymede and by including variability with local time, our functional fits quantitatively improve on the data-model agreement and provide a simple functional form for the magnetic field conditions near Ganymede.

4. Magnetospheric conditions at the time of Juno's Ganymede flyby

Juno's close Ganymede flyby occurred on 7 June 2021, with closest approach at 16:56 UT at a subspacecraft SIII right handed longitude of 57.5º (Hansen et al., this issue). The spacecraft encountered Ganymede's magnetosphere and wake at SIII right handed longitudes ~70º to ~50º, when Ganymede was just south of the magnetic equator and very close to the center of the plasma sheet. (A radial distance of 15 R_J at the jovigraphic equator and SIII longitudes 50º to 70º corresponds to magnetic latitudes of -4.1º to 0.7º and z_{mag} from -1.07 R_J to -0.16 R_J.) We follow three steps in estimating the magnetic field conditions upstream of Ganymede.

First, we consider the predicted conditions using the JRM09 + CON2020 average and temporally varying model. The JRM09 + CON2020 model (with average current constant values) predicts the following field values for SIII longitudes 50º-70º (see Table 2): B_R ~ -29 nT to ~0 nT, B_θ ~ 69 nT, B_φ ~ -10 nT to -13 nT, $|B|$ ~ 76 nT to 71 nT, bendback angle ~ 20º-85º, and elevation angle ~ 70º-89º. At those longitudes, using the largest or smallest best fit values of the CON2020 current constants rather than the average values would change the modeled field components roughly as follows: $B_R \pm 1$ nT, $B_\theta \pm 6$ nT, $B_\varphi \pm 1$ nT, $|B| \pm 5$ nT. This gives us the full range of expected field conditions at the time of Juno's Ganymede flyby and shows that the individual field components and field magnitude can vary by as much as ±5-10 percent of their average values.

Second, we fit the data to the CON2020 model to obtain a rough estimate of the best fit current constants to evaluate the state of the magnetosphere during orbit 34. We followed Vogt et al. (2017) in varying only the $\frac{\mu_0 I_0}{2}$ parameter to fit B_θ, at radial distances 10 to 30 R_J during each orbit's inbound pass and excluding the Ganymede flyby interval during orbit 34. We then fit the measured B_φ by varying the radial current constant value with the best fit $\mu_0 I_0$ calculated for each orbit. For both $\frac{\mu_0 I_0}{2}$ and I_{rad} we estimated the best fit by calculating the model field at a range of values (with a 2 nT step size) and minimizing the root mean square error between the external (measured – JRM09 internal field) and model field. Though our approach differs slightly from Connerney et al. (2020) we obtained nearly identical best fit $\mu_0 I_0$ values for Juno's first 24 orbits (see Figure S5), which gives us confidence in the validity of our fits estimates. We found that the first 34 Juno orbits featured an average $\frac{\mu_0 I_0}{2}$ fit of 144.3 nT (standard deviation 8.5 nT), consistent with the average 140.2 nT Connerney et al. (2020) reported from Juno's first 24 orbits. For orbit 34 we calculated a best fit $\frac{\mu_0 I_0}{2}$ fit of 138 nT, slightly below average. Our calculated best fit I_{rad} was 44 MA, though we note that the goodness of the B_φ fit was nearly independent of the radial current constant in orbit 34 and that our fit approach closely reproduced the Connerney et al. (2020) $\frac{\mu_0 I_0}{2}$ fit value but not the I_{rad} (our average was 23.8 MA, compared to 16.7 MA from Connerney et al. (2020); see Figure S6).

Finally, we compare the field measured by Juno during orbit 34 to the Galileo average along Juno's trajectory in magnetic coordinates, as shown in Figure 5. The black lines show Juno orbit 34 data as a function of ρ_{mag}, while the red lines in each panel show the Galileo average magnetic field values in each (ρ_{mag}, z_{mag}) bin from Figure 4 along Juno's trajectory (thick white line in Figure 4), and error bars show the standard deviation within the bins. This comparison shows that the magnetic field conditions in Jupiter's magnetosphere immediately before and after Juno's close Ganymede flyby were, overall, within the range of the typical Galileo measurements. The Juno field magnitude is typically slightly smaller than the Galileo averages, due in part to differences in B_φ, which is highly variable in this area. However, the Juno B_θ values are also systematically slightly smaller than the Galileo averages, which is consistent with Connerney et al. (2020)'s finding that the Juno-era height-integrated current in the magnetodisk is ~15% smaller than in the Pioneer, Voyager, and Galileo eras.

Overall, we find that the magnetic field measurements near Ganymede's orbit from Juno orbit 34 are well-described by the JRM09 internal field plus the *average* CON2020 model external field (blue lines in Figure 5). Only the B_φ component is systematically poorly fit by both the average Galileo field and by the JRM09+CON2020 model; the model field predicts B_φ ~ -11 nT at Ganymede though the observed B_φ is ~ -14 nT. The average model would therefore provide a good estimate of Jupiter's magnetospheric field during the flyby, though a better fit would use the slightly modified current constant parameters and would manually adjust the B_φ fit. Overall, the measured $|B|$ near Ganymede's orbit during Juno orbit 34 differs from the average JRM09+CON2020 model $|B|$ by only about ~2 percent and there is no systematic offset in $|B|$ or in B_θ as one would expect if the magnetodisk currents were significantly different from their average values.

5. Conclusions and Summary

The magnetic field conditions upstream of Ganymede display both spatial and temporal variability that can influence the moon-magnetosphere interaction. The spatial variability includes a local time dependence and, most significantly, a dependence on longitude due to Jupiter's ~10º dipole tilt. The longitudinal dependence is significantly larger than the observed orbit-to-orbit variability, with $|B|$ fluctuating from ~65 to ~125 nT during each planetary rotation. The field direction also varies significantly, with the bendback angle ranging from roughly -85º (almost completely swept back) to +85º (almost completely swept forward) and the elevation angle ranging from ~35º to ~90º (completely southward).

Galileo data from near the jovigraphic equator show that the longitudinal dependence of the magnetic field near Ganymede's orbit is well-described by the combined JRM09 internal field model (Connerney et al., 2018) and CON2020 external field model (Connerney et al., 2020), which computes the field due to Jupiter's current sheet. The CON2020 model includes azimuthal and radial current constant parameters that can be fit to data from each Galileo or Juno orbit to obtain a measure of the variability in Jupiter's magnetodisk. The expected orbit-to-orbit temporal variability obtained from these current sheet fits represents a ~10-20 percent variability in the baseline values of the individual field components and $|B|$, though the exact details depend on longitude. This possible variability should be considered when making preparations, such as reanalysis of Galileo flyby data or modeling work, for the upcoming NASA Europa Clipper and ESA JUICE missions.

During orbit 34, Juno flew past Ganymede at SIII right handed longitudes ~70º to ~50º, when Ganymede was just south of the magnetic equator and very close to the center of the plasma sheet. At these longitudes the expected average field conditions based on the JRM09+CON2020 model would be: B_R ~ -29 nT to ~0 nT, B_θ ~ 69 nT, B_φ ~ -10 nT to -13 nT, $|B|$ ~ 76 nT to 71 nT, bendback angle ~ 20º-85º, and elevation angle ~ 70º-89º. We calculated the best fit current constant parameters to Juno magnetic field data from orbit 34 and also compared the magnetic field along Juno's trajectory to Galileo averages from the same positions in magnetic coordinates. Our analysis showed that Jupiter's magnetospheric field during orbit 34 was very close to its average state. Overall, the orbit 34 data near Ganymede's orbit are well-described by the JRM09+CON2020 average model, with only the B_φ component being systematically underestimated in magnitude (predicted -11 nT compared to -14 nT observed). We look forward to future Juno, Europa Clipper, and JUICE data from Jupiter's inner magnetosphere that should provide new insight into the nature and causes of the temporal variability in Jupiter's magnetodisk and its influence on the plasma environments of the Galilean satellites.

Appendix A: Functional fits to magnetic field data near Ganymede

We have derived simple functional fits to the Galileo magnetic field measurements near Ganymede, including all data from radial distances 14.95-15.05 R_J (i.e. the data presented in Figure 2) except orbit C9, which occurred near 50º longitude, when B_θ and $|B|$ were anomalously small due to a likely current sheet crossing. At Ganymede's orbit the internal magnetic field is very well-approximated by a dipole field; at a radial distance of 15 R_J in the jovigraphic equator the longitudinally-average difference between the full JRM09 field model and the JRM09 dipole field (same tilt and dipole moment) is just ~1.5 percent of the field magnitude. We therefore chose to represent the field near Ganymede as the sum of a tilted dipole – using the values for the dipole moment and tilt from the JRM09 model – and an external field that does not depend on magnetic longitude but does vary with local time.

Based on qualitative and rough quantitative assessments of how the Galileo data and the CON2020 external field vary spatially, we chose the following functional forms for the magnetic field in cylindrical magnetic coordinates:

$$B_{\rho,ext} = \frac{z}{\sqrt{\rho}}(A + B\cos(\psi - C)) \quad \text{(A1)}$$

$$B_{\phi,ext} = \frac{z}{\rho}(D + E\cos(\psi - F)) \quad \text{(A2)}$$

$$B_{z,ext} = \frac{1}{\rho}(G + H\cos(\psi - I)) \quad \text{(A3)}$$

where A, B, C, D, E, F, G, H, and I are constants to be obtained by fitting, ρ and z are cylindrical magnetic coordinates in Jovian radii (R_J), ψ is local time in radians, and all field components are in units of nT. We note that parameters B, E, and H indicate the magnitude of the local time dependence of $B_{\rho,ext}$, $B_{\phi,ext}$, and $B_{z,ext}$, respectively, while C, F, and I indicate the phase of the local time dependence.

We first estimated the measured external field by subtracting the JRM09 dipole field from the observed magnetic field values. We then fit the measured external field components to eqs. 1-3 using the IDL function curvefit, obtaining the following values for the fit parameters: A = 49.87, B = 6.41, C = 4.74 hours, D = -6.87, E = -8.93, F = 6.88 hours, G = 707.98 nT, H = -133.38 nT, I = 14.80 hours. The magnitude of the local time dependence is ~10-20 percent of the background value for $B_{\rho,ext}$, $B_{z,ext}$ but substantially larger for $B_{\phi,ext}$, probably because of the relatively large amount of scatter in B_{φ} (see Figure 4). The magnitude of $B_{\rho,ext}$ and $B_{\phi,ext}$ both peak near dawn, consistent with observations showing a more radially stretched field and thin current sheet near dawn than near dusk (e.g. Palmaerts et al., 2017). The minimum in $B_{z,ext}$, which corresponds to the peak in B_θ, occurs near 15:00 LT, which is consistent with the 2-D fit of Vogt et al. (2011).

Table A1 compares the RMS error between the Galileo measurements and the functional fits we have derived here to the RMS error obtained using JRM09 with either CON2020 or the Khurana (1997) external field. Though this functional fit is only applicable very close to Ganymede's orbit (15 R_J at the jovigraphic equator), it does a substantially better job of matching the B_θ field component, and reduces the RMS error for B_φ and $|B|$, compared to both field models. The 7.76 nT RMS error in $|B|$ represents a ~7.7 percent error in the average measured $|B|$.

Figure A1 shows our functional fits, rotated into SIII coordinates, as a function of longitude. The field was evaluated at 15 R_J in the jovigraphic equator as a function of longitude at noon (blue) and midnight (red) local times and is plotted along with the average CON2020 field (black solid lines) and Khurana (1997) model field (black dashed lines). The magnitude and longitudinal profile of our functional fit and CON2020 are very similar.

For both Galileo and Juno, the measured magnetic field and its spatial dependence is commonly expressed in SIII coordinates, though we calculated our functional fit in magnetic cylindrical coordinates. Therefore, we briefly describe here the equations needed to rotate from magnetic to SIII coordinates. The rotation from SIII spherical coordinates (r, θ, φ) to cartesian magnetic coordinates (x_{mag}, y_{mag}, z_{mag}) where z_{mag} is aligned with the dipole axis, which is tilted by an angle θ_d toward jovigraphic longitude φ_d, and x_{mag} points toward jovigraphic longitude φ_d, is given by:

$$x_{mag} = r[\sin\theta\cos(\varphi - \varphi_d)\cos\theta_d - \cos\theta\sin\theta_d] \quad \text{(A4)}$$

$$y_{mag} = r\sin\theta\sin(\varphi - \varphi_d) \quad \text{(A5)}$$

$$z_{mag} = r[\cos\theta\cos\theta_d + \sin\theta\cos(\varphi - \varphi_d)\sin\theta_d] \quad \text{(A6)}$$

For the JRM09 dipole, θ_d = 10.31º and φ_d = 163.39º in right-handed longitude.

The full magnetic field of the functional fit is calculated by adding the dipole and external field components in magnetic cylindrical coordinates:

$$B_\rho = B_{\rho,dipole} + B_{\rho,ext} \quad \text{(A7)}$$

$$B_\phi = B_{\phi,dipole} + B_{\phi,ext} \quad \text{(A8)}$$

$$B_z = B_{z,dipole} + B_{z,ext} \quad \text{(A9)}$$

The dipole field can be calculated from the usual equations using the JRM09 dipole moment M = 4.170 G (Connerney et al., 2018). The simplest way to rotate the field from magnetic cylindrical coordinates to SIII cartesian coordinates is to first convert from magnetic cylindrical coordinates to magnetic cartesian coordinates ($B_{x,mag}$, $B_{y,mag}$, $B_{z,mag}$) then rotate into SIII cartesian coordinates following:

$$B_{x,SIII} = \left(B_{x,mag}\cos\theta_d + B_{z,mag}\sin\theta_d\right)\cos\varphi_d - B_{y,mag}\sin\varphi_d \quad \text{(A10)}$$

$$B_{y,SIII} = B_{y,mag}\cos\varphi_d + \left(B_{x,mag}\cos\theta_d + B_{z,mag}\sin\theta_d\right)\sin\varphi_d \quad \text{(A11)}$$

$$B_{Z,SIII} = B_{z,mag}\cos\theta_d - B_{x,mag}\sin\theta_d\ . \quad \text{(A12)}$$

Finally, the field can then be converted from SIII cartesian to SIII spherical coordinates using the typical equations.

Acknowledgements

We gratefully acknowledge helpful discussions with Jack Connerney and constructive comments from Xianzhe Jia and an anonymous reviewer. The JRM09 + CAN2020 current sheet code used to create several figures was developed by M.F.V. in collaboration with Rob Wilson, Gabby

Provan, Matt James, and Marty Brennan and is available at https://github.com/rjwilson-LASP/PSH and https://github.com/marissav06/con2020_idl. Magnetometer data from all spacecraft that have visited the Jovian system are available from the Planetary Data System. Specifically, Galileo data can be downloaded from https://pds-ppi.igpp.ucla.edu/search/?sc=Galileo&t=Jupiter&i=MAG, and Juno data can be downloaded from https://pds-ppi.igpp.ucla.edu/search/?sc=Juno&t=Jupiter&i=FGM. M.F.V. was supported by NASA grant 80NSSC20K0559 and by the Juno Participating Scientist program.

References

Bagenal, F., & Dols, V. (2020). The space environment of Io and Europa. Journal of Geophysical Research: Space Physics, 125, e2019JA027485. https://doi.org/10.1029/2019JA027485

Behannon, K. W., L. F. Burlaga, and N. F. Ness (1981), The Jovian magnetotail and its current sheet, *J. Geophys. Res.*, *86*, 8385-8401.

Bolton, S.J., Lunine, J., Stevenson, D. et al. Space Sci Rev (2017) 213: 5. https://doi.org/10.1007/s11214-017-0429-6

Connerney, J., M. Acuña, and N. Ness (1981), Modeling the Jovian Current Sheet and Inner Magnetosphere, *J. Geophys. Res.*, *86*(A10), 8370-8384.

Connerney, J.E.P., Benn, M., Bjarno, J.B., Denver, T., Espley, J., Jorgensen, J.L., et al. (2017). The Juno magnetic field investigation, Space Sci. Rev., 213(1-4), 39-138, doi: 10.1007/s11214-017-0334-z.

Connerney, J. E. P., Kotsiaros, S., Oliversen, R. J., Espley, J. R., Joergensen, J. L., Joergensen, P. S., et al. (2018). A new model of Jupiter's magnetic field from Juno's first nine orbits. Geophysical Research Letters, 45. https://doi.org/10.1002/2018GL077312

Connerney, J. E. P., Timmins, S., Herceg, M., & Joergensen, J. L. (2020). A Jovian magnetodisc model for the Juno era. *Journal of Geophysical Research: Space Physics*, *125*, e2020JA028138. https://doi.org/10.1029/2020JA028138

Hansen, C. J, et al., Juno's Close Encounter with Ganymede – an Overview, submitted to Geophys. Res. Lett., this issue.

Jia, X., Walker, R. J., Kivelson, M. G., Khurana, K. K., and Linker, J. A. (2009), Properties of Ganymede's magnetosphere inferred from improved three-dimensional MHD simulations, J. Geophys. Res., 114, A09209, doi:10.1029/2009JA014375.

Jia, X., Walker, R. J., Kivelson, M. G., Khurana, K. K., and Linker, J. A. (2010), Dynamics of Ganymede's magnetopause: Intermittent reconnection under steady external conditions, J. Geophys. Res., 115, A12202, doi:10.1029/2010JA015771.

Kaweeyanun, N., Masters, A., & Jia, X. (2020). Favorable conditions for magnetic reconnection at Ganymede's upstream magnetopause. Geophysical Research Letters, 47, e2019GL086228. https://doi.org/10.1029/2019GL086228

Khurana, K. K. (1997), Euler potential models of Jupiter's magnetospheric field, *J. Geophys. Res.*, *102*(A6), 11295-11306.

Kivelson, M. G., K. K. Khurana, C. T. Russell, R. J. Walker, J. Warnecke, F. V. Coroniti, C. Polanskey, D. J. Southwood, and G. Schubert (1996), Discovery of Ganymede's magnetic field by the Galileo spacecraft, *Nature, 384,* 537 - 541.

Kivelson, M. G., Khurana, K. K., Stevenson, D. J., Bennett, L., Joy, S., Russell, C. T., Walker, R. J., Zimmer, C., and Polanskey, C. (1999), Europa and Callisto: Induced or intrinsic fields in a periodically varying plasma environment, J. Geophys. Res., 104(A3), 4609– 4625, doi:10.1029/1998JA900095.

Kivelson, M.G., Khurana, K. K., & Volwerk, M. (2002), The permanent and inductive magnetic moments of Ganymede, Icarus, 157, 507–522, doi:10.1006/icar.2002.6834.

Kivelson, M. G. et al., “Ganymede: Its Magnetosphere and its Interaction with the Jovian Magnetosphere”, in: “Ganymede”, eds. M. Volwerk, M. McGrath, X. Jia and T. Spohn, Cambridge University Press, Cambridge, UK, pre-press, 2022.

Louarn, P., C. P. Paranicas, and W. S. Kurth (2014), Global magnetodisk disturbances and energetic particle injections at Jupiter, *J. Geophys. Res. Space Physics*, *119*, 4495–4511, doi:10.1002/2014JA019846.

Mauk, B. H., D. J. Williams, R. W. McEntire, K. K. Khurana, and J. G. Roederer (1999), Storm-like dynamics of Jupiter's inner magnetosphere, *J. Geophys. Res*., *104*, 22,759.

Palmaerts, B., Vogt, M. F., Krupp, N. , Grodent, D. and Bonfond, B. (2017). Dawn-Dusk Asymmetries in Jupiter's Magnetosphere. In Dawn-Dusk Asymmetries in Planetary Plasma Environments (eds S. Haaland, A. Runov and C. Forsyth). doi:10.1002/9781119216346.ch24

Phipps, P., & Bagenal, F. (2021). Centrifugal equator in Jupiter's plasma sheet. Journal of Geophysical Research: Space Physics, 126, e2020JA028713., DOI: https://doi.org/10.1029/2020JA028713

Russell, C. T., Z. J. Yu, K. K. Khurana, and M. G. Kivelson (2001), Magnetic field changes in the inner magnetosphere of Jupiter, *Adv. Space Res.*, *28*(6), 897-902.

Tao, C., R. Kataoka, H. Fukunishi, Y. Takahashi, and T. Yokoyama (2005), Magnetic field variations in the Jovian magnetotail induced by solar wind dynamic pressure enhancements, *J. Geophys. Res.*, *110*, A11208, doi:10.1029/2004JA010959.

Tóth, G., Jia, X., Markidis, S., Peng, I. B., Chen, Y., Daldorff, L. K. S., Tenishev, V. M., Borovikov, D., Haiducek, J. D., Gombosi, T. I., et al. (2016), Extended magnetohydrodynamics with embedded particle-in-cell simulation of Ganymede's magnetosphere, J. Geophys. Res. Space Physics, 121, 1273– 1293, doi:10.1002/2015JA021997.

Vogt, M. F., E. J. Bunce, J. D. Nichols, J. T. Clarke, and W. S. Kurth (2017), Long-term variability of Jupiter's magnetodisk and implications for the aurora, Journal of Geophysical Research: Space Physics, 122, 12,090–12,110, doi:10.1002/2017JA024066.

Vogt, M. F., Gyalay, S., Kronberg, E. A., Bunce, E. J., Kurth, W. S., Zieger, B., & Tao, C. (2019). Solar wind interaction with Jupiter's magnetosphere: A statistical study of Galileo in situ data and modeled upstream solar wind conditions. Journal of Geophysical Research: Space Physics, 124, 10170– 10199. https://doi.org/10.1029/2019JA026950

Zhou, H., Tóth, G., Jia, X., & Chen, Y. (2020). Reconnection-driven dynamics at Ganymede's upstream magnetosphere: 3-D global Hall MHD and MHD-EPIC simulations. Journal of Geophysical Research: Space Physics, 125, e2020JA028162. https://doi.org/10.1029/2020JA028162

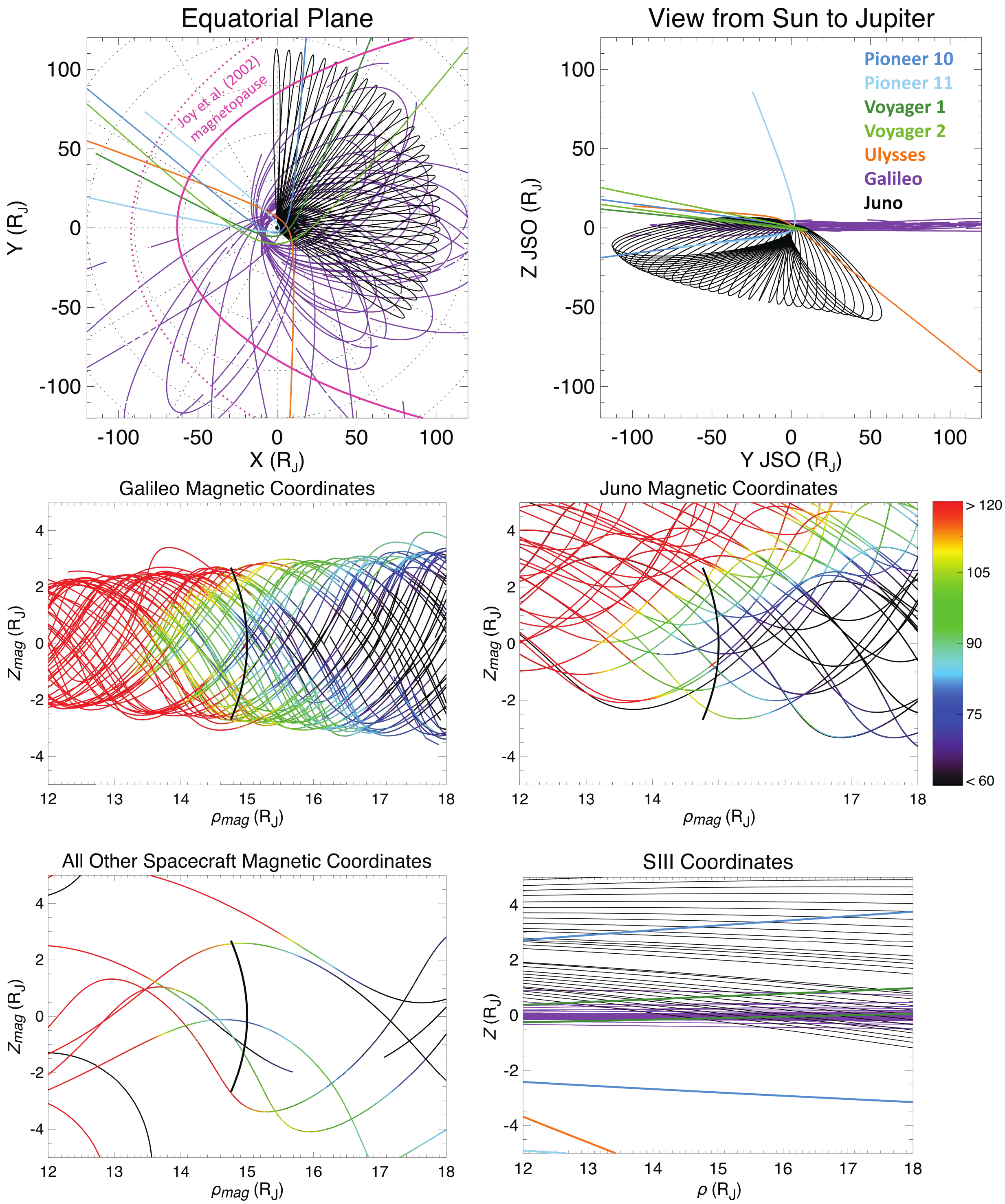

Figure 1. Trajectories of all spacecraft that have visited Jupiter's magnetosphere except Cassini and New Horizons. Top left: spacecraft trajectories projected onto the equatorial plane, with the Joy et al. (2002) magnetopause boundaries in pink. Top right: spacecraft trajectories as viewed

from the sun in JSO coordinates. Middle left: “wiggle plot” showing Galileo’s orbital coverage near Ganymede’s orbit, plotted in JRM09 magnetic cylindrical coordinates with color indicating the measured magnetic field magnitude. The thick black line shows the possible range of Ganymede’s location (15 R_J radial distance and 0º jovigraphic latitude). Middle right: “wiggle plot” showing Juno’s orbital coverage near Ganymede’s orbit, plotted in JRM09 magnetic cylindrical coordinates. Bottom left: “wiggle plot” showing trajectories of Pioneers 10 and 11, Voyagers 1 and 2, and Ulysses near Ganymede’s orbit, plotted in JRM09 magnetic cylindrical coordinates. Bottom right: spacecraft trajectories in System III cylindrical coordinates near Ganymede’s orbit.

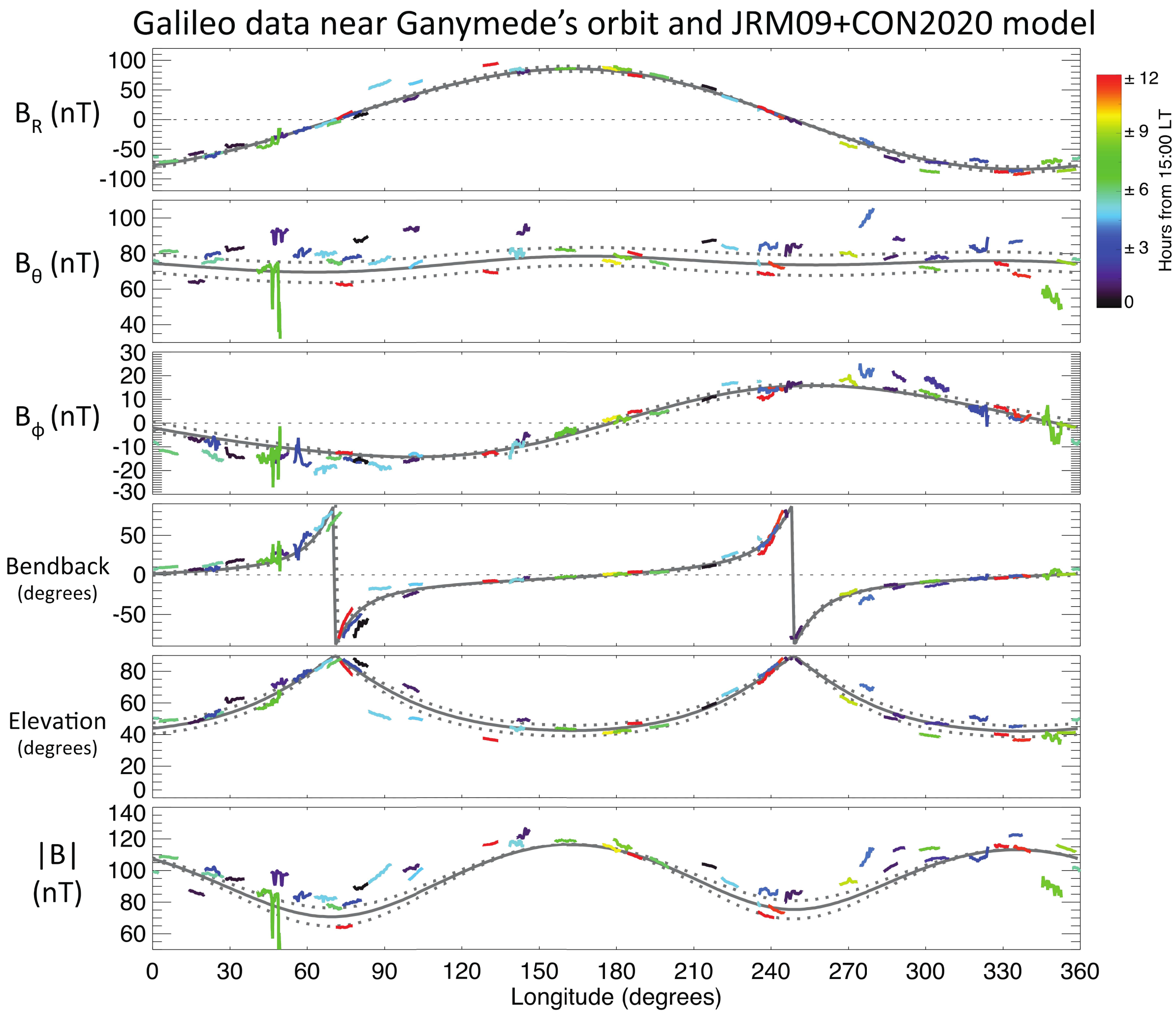

Figure 2. Dependence of the magnetic field near Ganymede's orbit as a function of System III right-handed longitude, as measured by Galileo at radial distances 14.95-15.05 R_J, excluding the spacecraft's six close flybys of Ganymede. From top: the radial (B_R), meridional (B_θ), and azimuthal (B_φ) components of the magnetic field in nT, the field bendback and elevation angles in degrees, and the field magnitude ($|B|$) in nT. Color indicates the number of hours of local time from 15:00. Gray solid lines show the field predicted by the average JRM09 + CON2020 model (Connerney et al., 2018, 2020) at Ganymede's orbit while the dashed lines show the range of the expected field conditions based on model fits to individual Juno orbits (Connerney et al., 2020).

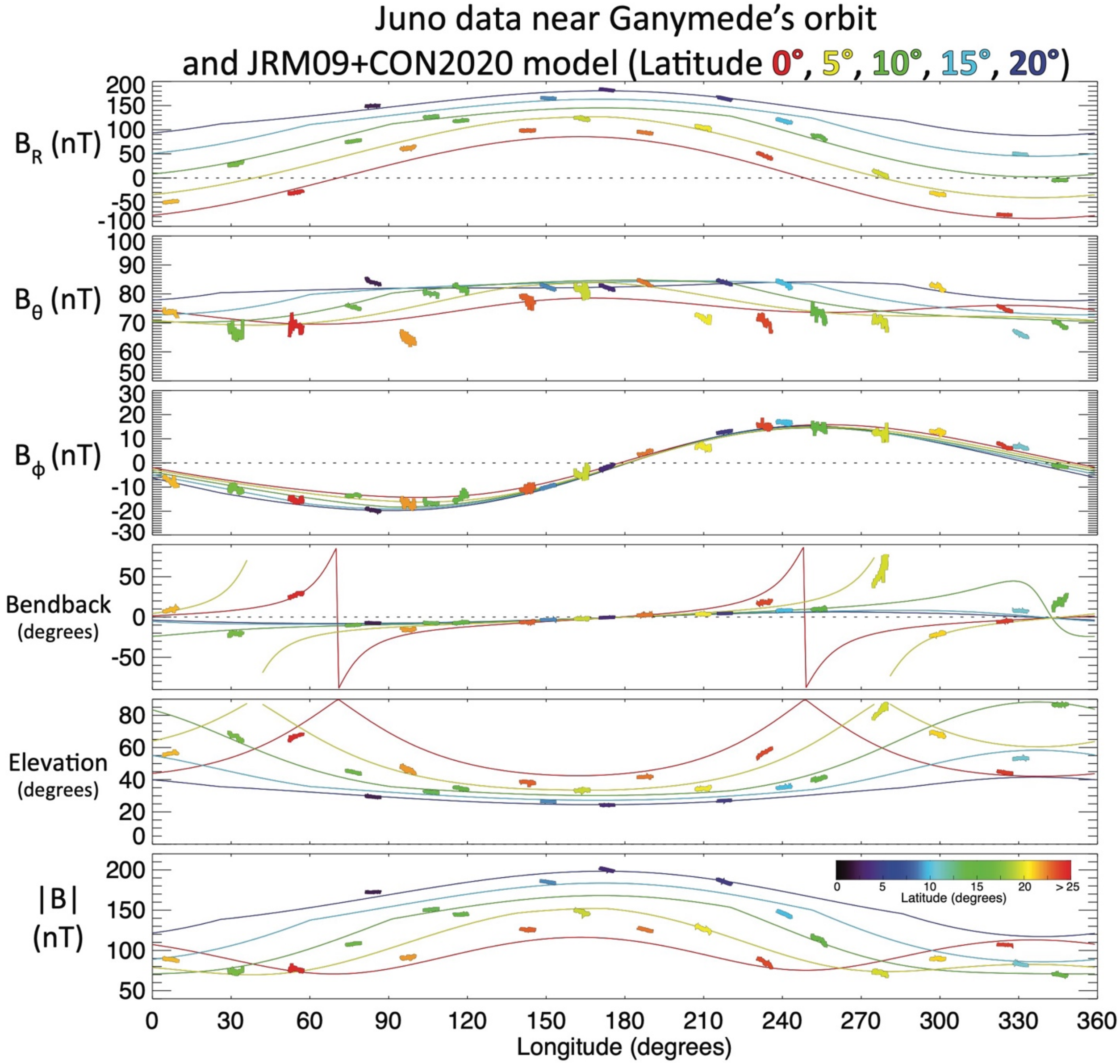

Figure 3. Dependence of the magnetic field near Ganymede's orbit as a function of System III right-handed longitude, from Juno's first 33 orbits at radial distances 14.95-15.05 R_J. From top: the radial (B_R), meridional (B_θ), and azimuthal (B_φ) components of the magnetic field in nT, the field bendback and elevation angles in degrees, and the field magnitude $|B|$ in nT. Data from each orbit are plotted with color indicating the average jovigraphic latitude of the spacecraft during the interval shown. The red solid line in each panel shows the quantity predicted by the JRM09 + CON2020 model (Connerney et al., 2018, 2020) at 15 R_J at the jovigraphic equator, while

yellow, green blue, and purple lines show the model predictions at 5º, 10º, 15º, and 20º jovigraphic latitude, respectively.

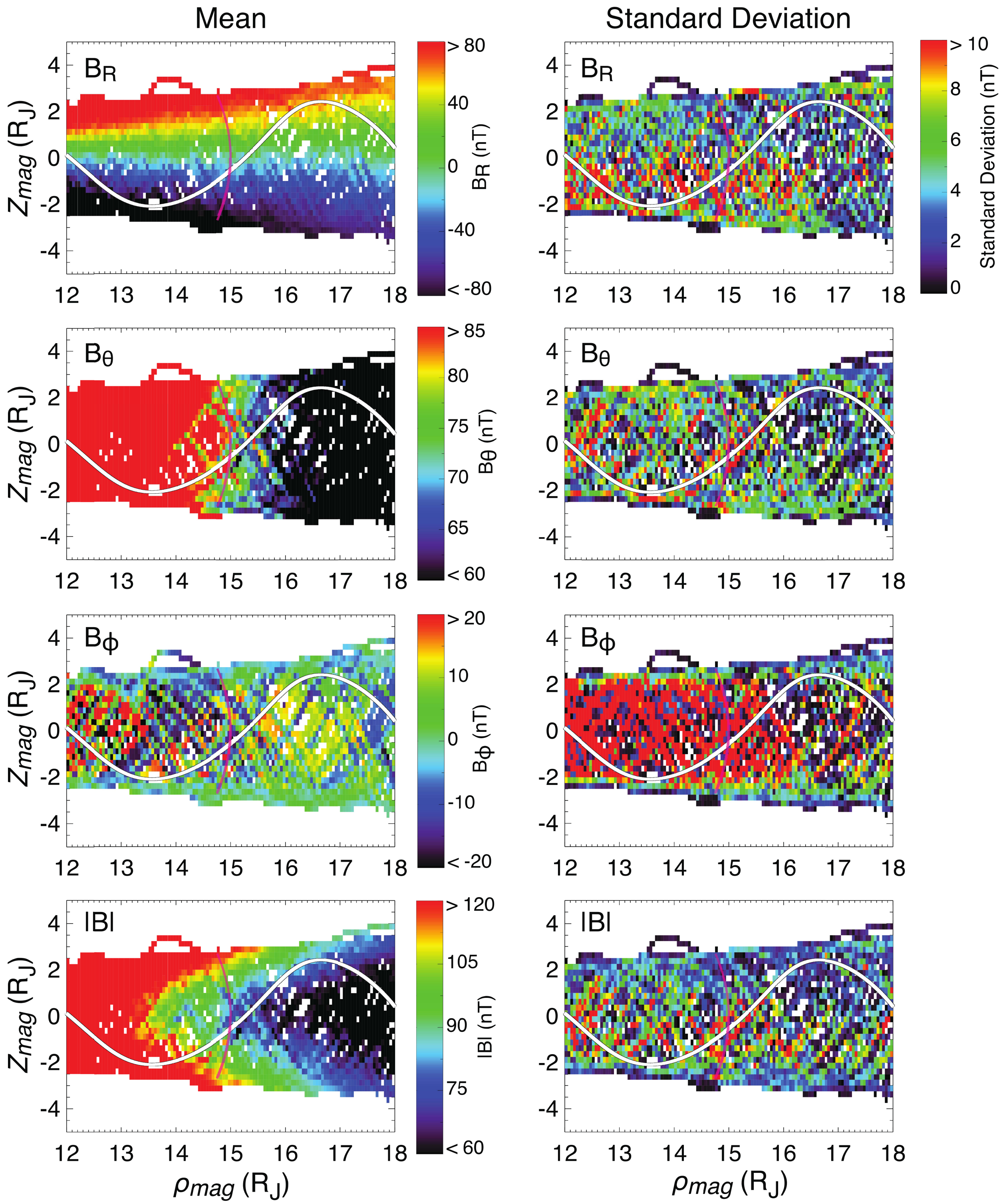

573

574 **Figure 4.** Magnetic field conditions measured by Galileo near Ganymede's orbit, organized in

575 magnetic cylindrical coordinates. Boxes spanning 0.05 R_J in ρ_{mag} by 0.25 R_J in z_{mag} are drawn

with the color of each box indicating the mean measured magnetic field (left column) or standard deviation of the measured magnetic field (right column) in each box. Thick white lines in each panel show Juno's trajectory during orbit 34 and pink curves show the range of Ganymede's possible positions.

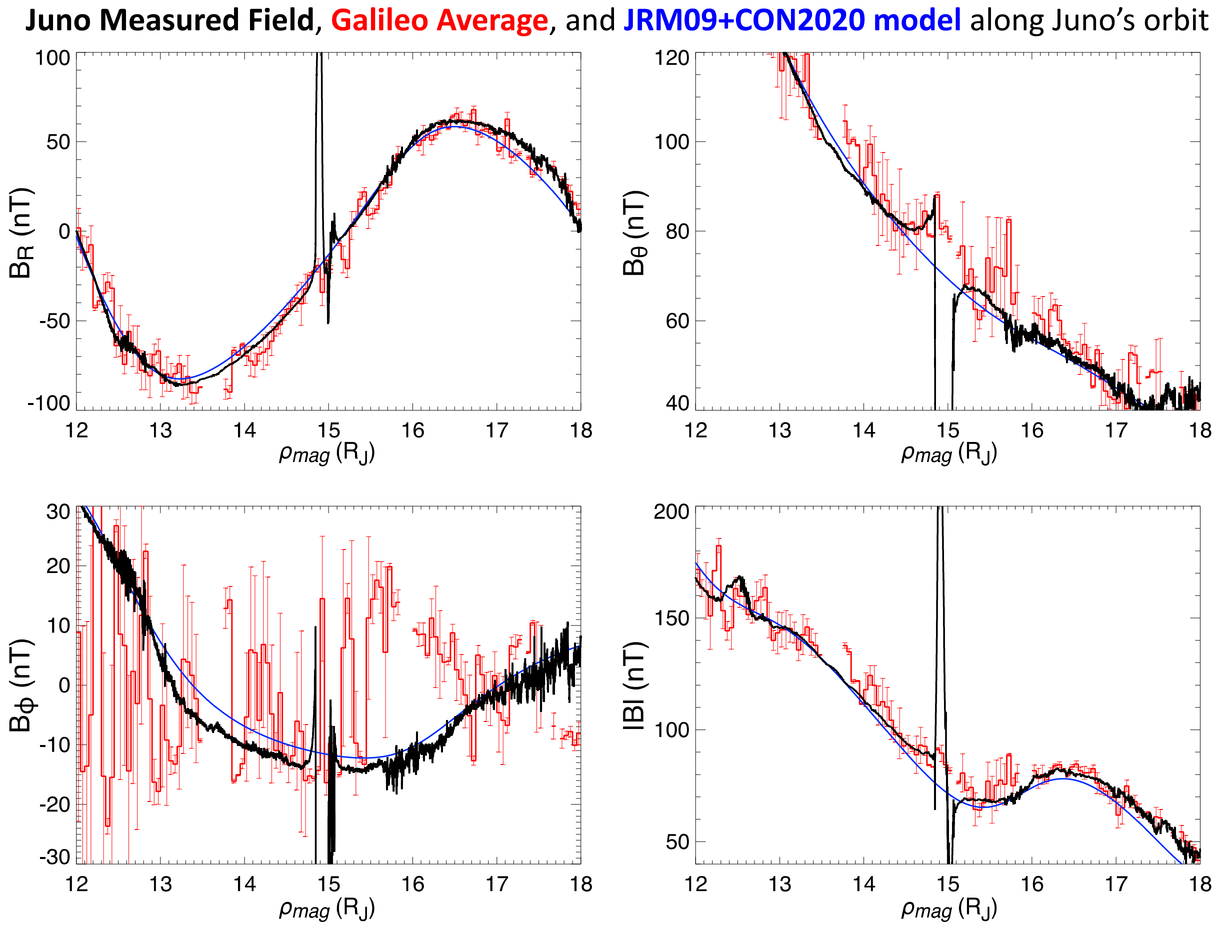

Figure 5. Magnetic field components and magnitude measured by Juno during orbit 34 as a function of magnetic cylindrical distance ρ_{mag}. Also shown in red are the average magnetic field measured by Galileo, with error bars indicating the standard deviation, along Juno's trajectory in magnetic coordinates, calculated in bins of 0.05 R_J in ρ_{mag} and 0.25 R_J in z_{mag}. Blue lines show the JRM09+CON2020 model field.

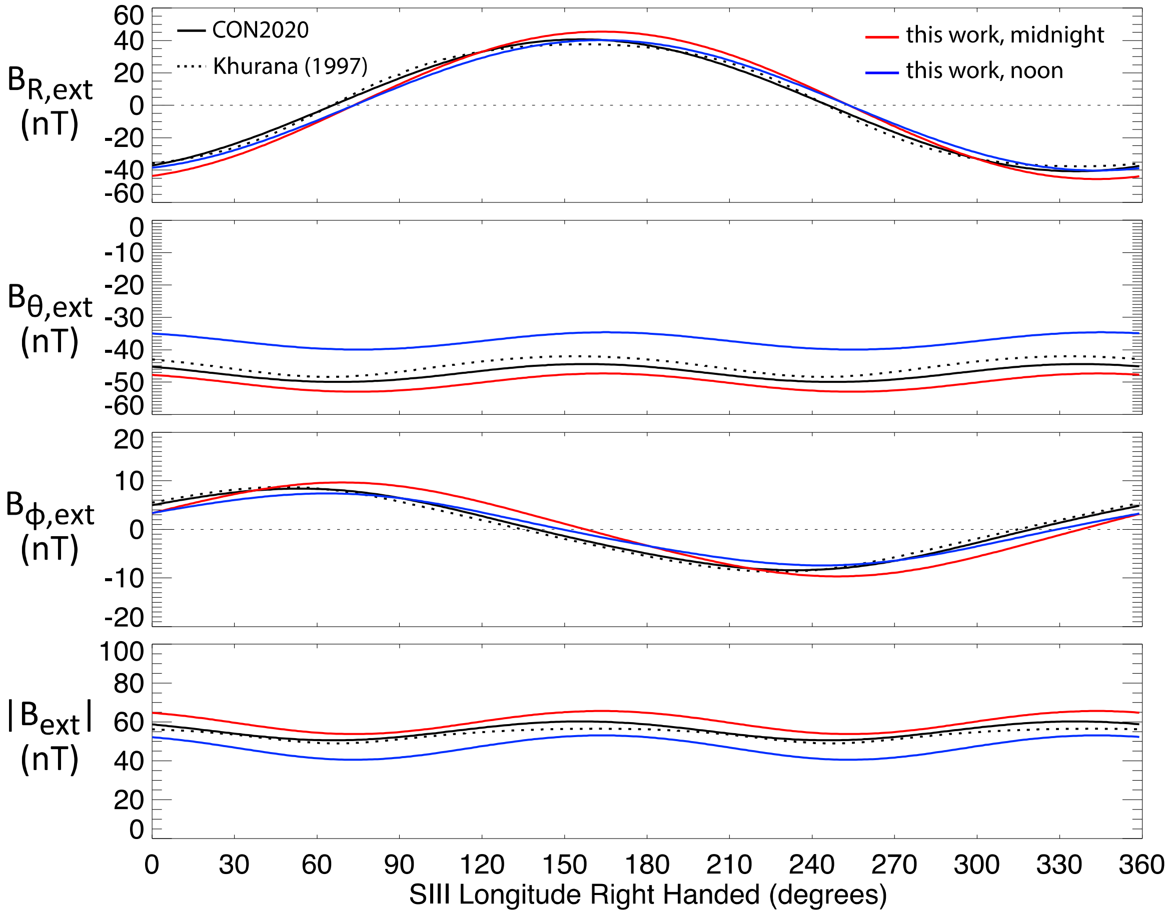

Figure A1. Modeled external field at radial distance 15 R_J in the jovigraphic equator from the CON2020 model (black solid lines), Khurana (1997) model (black dashed lines), and the functional fits described in equations A1-A3 evaluated at noon (blue) and midnight (red) local times, plotted as a function of longitude. From top: the radial (B_R), meridional (B_θ), and azimuthal (B_φ) components of the magnetic field, and the field magnitude ($|B|$), all in nT.

Table 1. Measured[a] and modeled magnetic field values and field angles near Ganymede's orbit

	Minimum (excepting orbit C9[b])	Maximum (all orbits)	Minimum (Orbit C9 only[a])	JRM09 + CON2020 model minimum[b]	JRM09 + CON2020 model maximum[b]	JRM09 + CON2020 model average[c,d]	Average variability due to change in CON2020 current constants[d]
B_R (nT)	-92.78	95.15		-83.80	85.61	53.9	~6 nT
$\boldsymbol{B_\theta}$ (nT)	48.50	105.50	32.06	69.54	78.55	74.36	~11 nT
$\boldsymbol{B_\varphi}$ (nT)	-21.91	25.12	-27.10	-14.28	15.83	9.47	~2 nT
$\|B\|$ (nT)	63.76	126.59	37.24	70.76	116.2	94.95	~5 nT
Bendback angle[e] (degrees)	-82.43	82.06		-88.43	86.62	17.39	~4º
Elevation angle[e] (degrees)	33.75	88.61		42.15	89.72	56.30	~6º

[a] Galileo measurements at radial distances 14.95-15.05 R_J excepting the six close flybys of Ganymede, at near-jovigraphic latitudes (-1.57º to 3.27º)

[b] The magnetic field measured during orbit C9, which occurred near 50º longitude, was anomalously small due to a likely current sheet crossing, which affects the minimum observed B_θ, B_φ, and $|B|$.

[c] Model values were calculated at 15.0 R_J, 0º latitude, and from 0º to 360º longitude in 1º increments, using the average CON2020 current constant fit values.

[d] Averages and variability are calculated using $|B_R|$, $|B_\varphi|$, and the magnitude of the field bendback angle.

[e] Field angles are not calculated when $|B_R| < 3$ nT.

Table 2. JRM09 + CON2020 model prediction at Ganymede's orbit[a] during the Juno flyby

	50º longitude, average	50º longitude, expected temporal variability	70º longitude, average	70º longitude, expected temporal variability
B_R (nT)	-28.3	-29.6 – -27.1	-1.1	-0.7 – -1.4
$\boldsymbol{B_\theta}$ (nT)	69.9	64.1 – 75.3	69.6	63.7 – 75.2
$\boldsymbol{B_\varphi}$ (nT)	-10.2	-8.7 – -11.4	-11.5	-11.7 – -13.4
$\|B\|$ (nT)	76.1	71.2 – 80.8	72.1	64.8 – 76.3
Bendback angle	19.9º	16.3º – 22.8º	37.5º	86.6º – 84.1º
Elevation angle (degrees)	67.9º	65.2º – 70.2º	77.9º	89.4º – 88.9º

[a]Model field computed at 15 R_J radial distance and 0º jovigraphic latitude

Table A1. Root mean square error between the field model and Galileo measurements at 14.95 $R_J < R < 15.05$ R_J (excepting orbit C9)

Model	B_R RMS Error (nT)	B_θ RMS Error (nT)	B_φ RMS Error (nT)	$\lvert B\rvert$ RMS Error (nT)
JRM09 (full model) + CON2020	7.12	9.24	3.42	8.93
JRM09 (full model) + Khurana (1997) with V2 parameters[a]	7.65	8.74	3.53	7.91
JRM09 dipole + this work	8.50	6.46	3.01	7.76
JRM09 full model + this work	8.03	6.01	3.17	7.11

[a] Khurana (1997) fit model parameters separately to Voyager 1, Voyager 2, and Pioneer 10 data and also provided a set of "common model" fit parameters obtained using data from all three spacecraft. For B_θ, B_φ, and $|B|$, the smallest RMS errors between Galileo data and the JRM09+K97 are obtained when using the V2 parameters and the largest RMS errors are obtained using the V1 parameters. For B_R, the "common model" parameters produce the smallest RMS

error (6.63 nT – though the overall $|B|$ RMS error is 10.29 nT) while the V2 parameters produce the largest RMS error.

Figure 1.

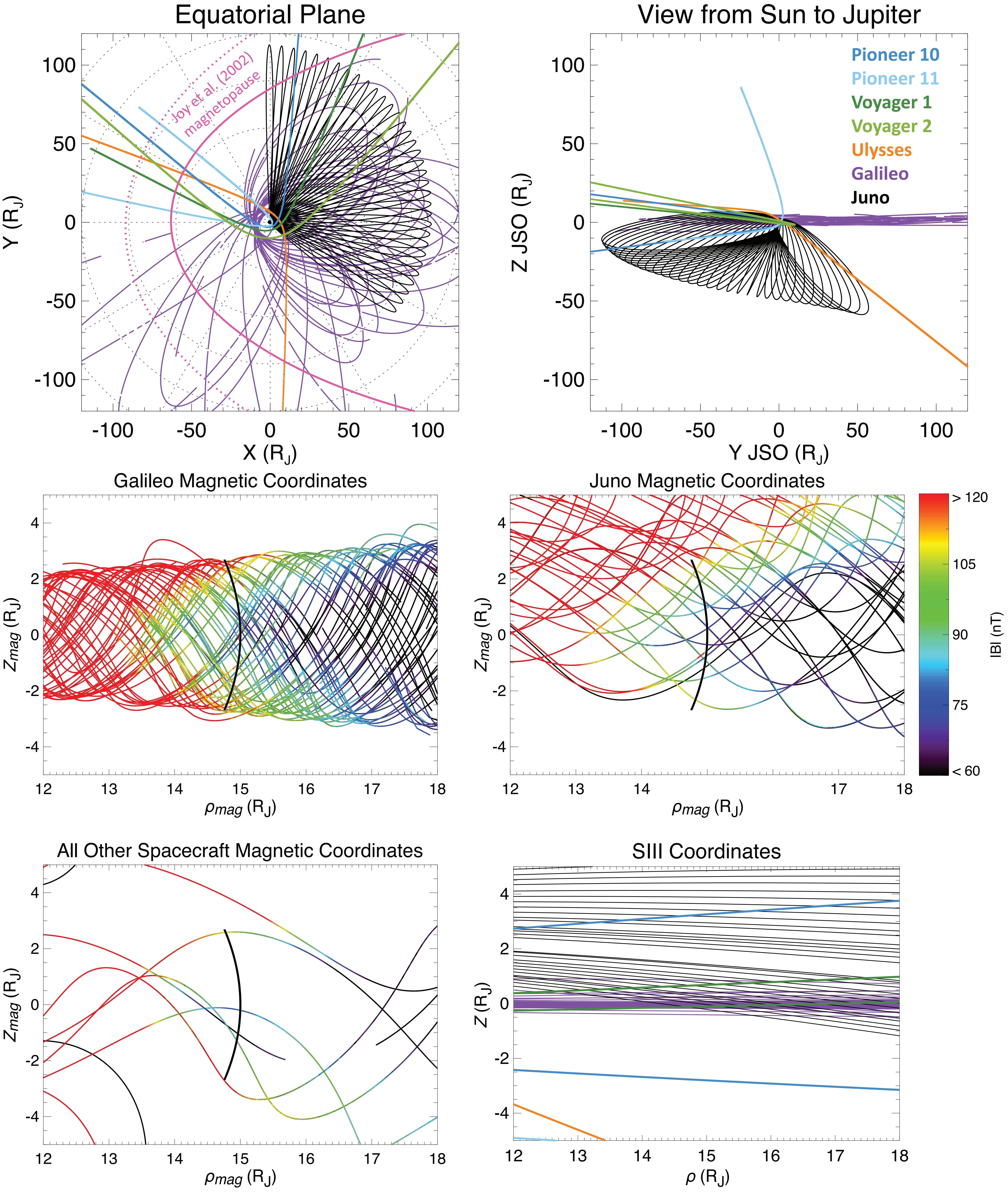

Equatorial Plane
Joy et al. (2002) magnetopause
Y (RJ)
X (RJ)
View from Sun to Jupiter
Pioneer 10
Pioneer 11
Voyager 1
Voyager 2
Ulysses
Galileo
Juno
Z JSO (RJ)
Y JSO (RJ)
Galileo Magnetic Coordinates
Juno Magnetic Coordinates
Zmag (RJ)
ρmag (RJ)
> 120
105
90
75
< 60
IBI (nT)
All Other Spacecraft Magnetic Coordinates
SIII Coordinates
Z (RJ)
ρ (RJ)

Figure 2.

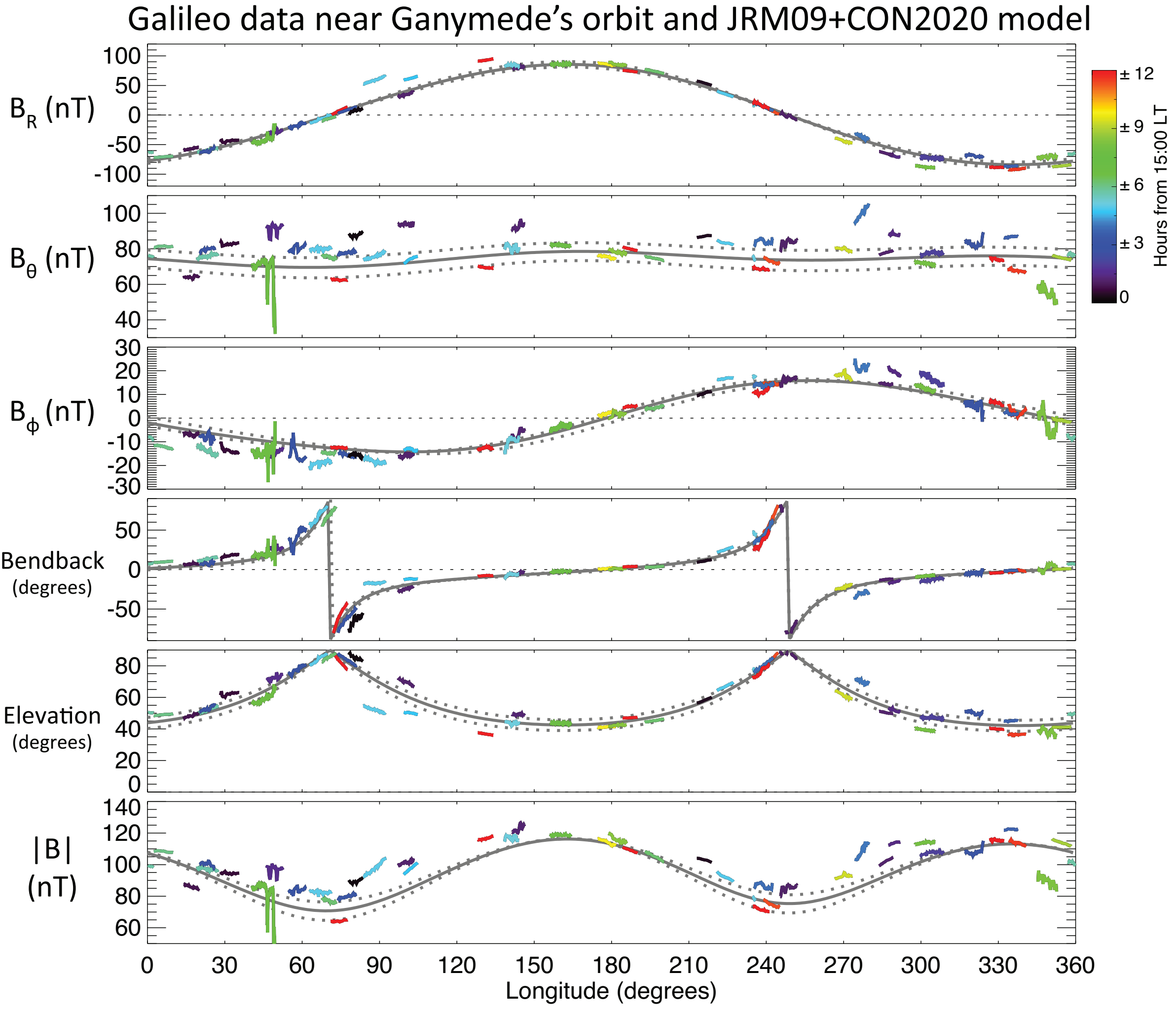

Galileo data near Ganymede's orbit and JRM09+CON2020 model
B_R (nT)
B_θ (nT)
B_φ (nT)
Bendback (degrees)
Elevation (degrees)
|B| (nT)
Longitude (degrees)
Hours from 15:00 LT
± 12
± 9
± 6
± 3
0

Figure 3.

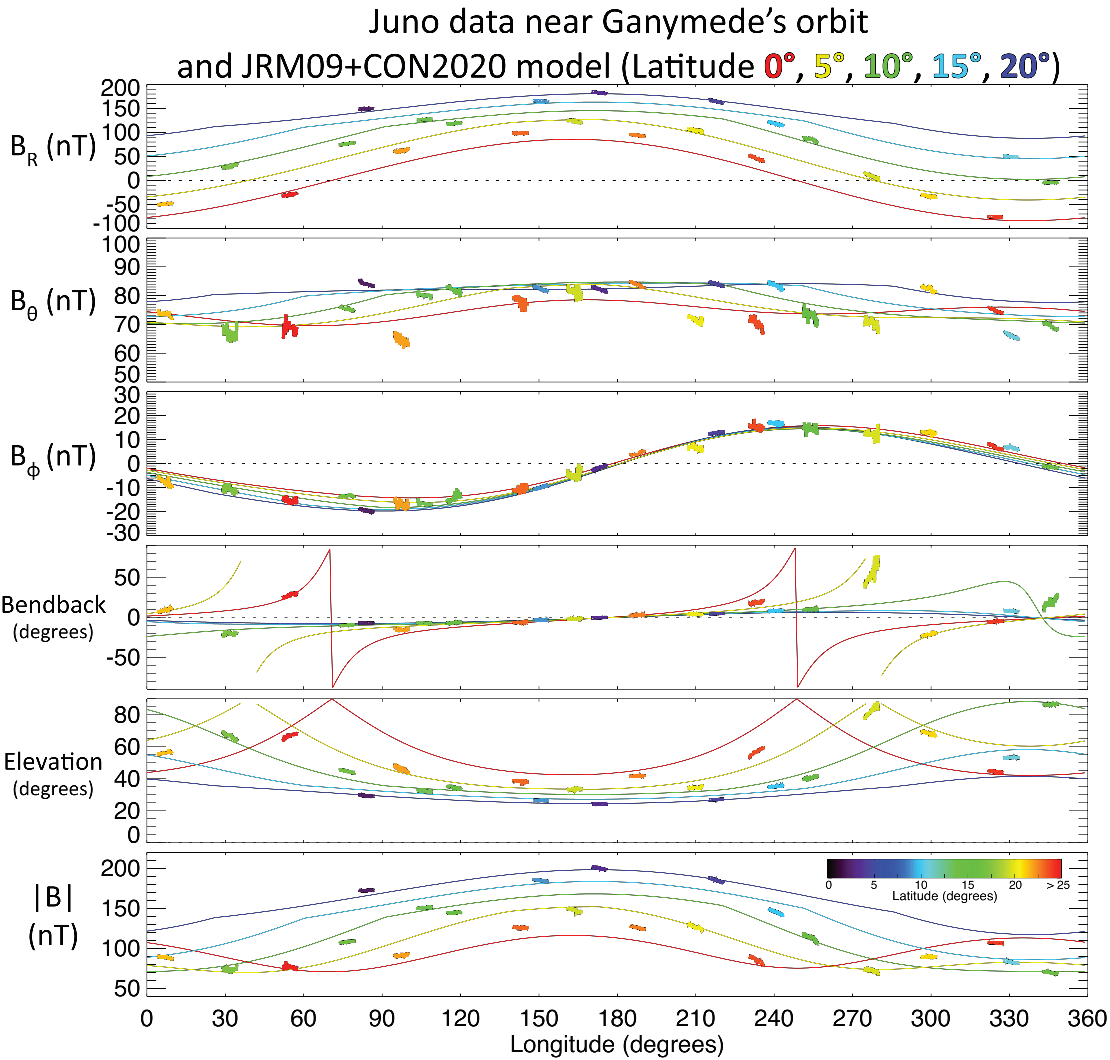

Juno data near Ganymede's orbit
and JRM09+CON2020 model (Latitude 0°, 5°, 10°, 15°, 20°)
B_R (nT)
B_θ (nT)
B_φ (nT)
Bendback
(degrees)
Elevation
(degrees)
|B|
(nT)
Latitude (degrees)
0 5 10 15 20 > 25
Longitude (degrees)
0 30 60 90 120 150 180 210 240 270 300 330 360

Figure 4.

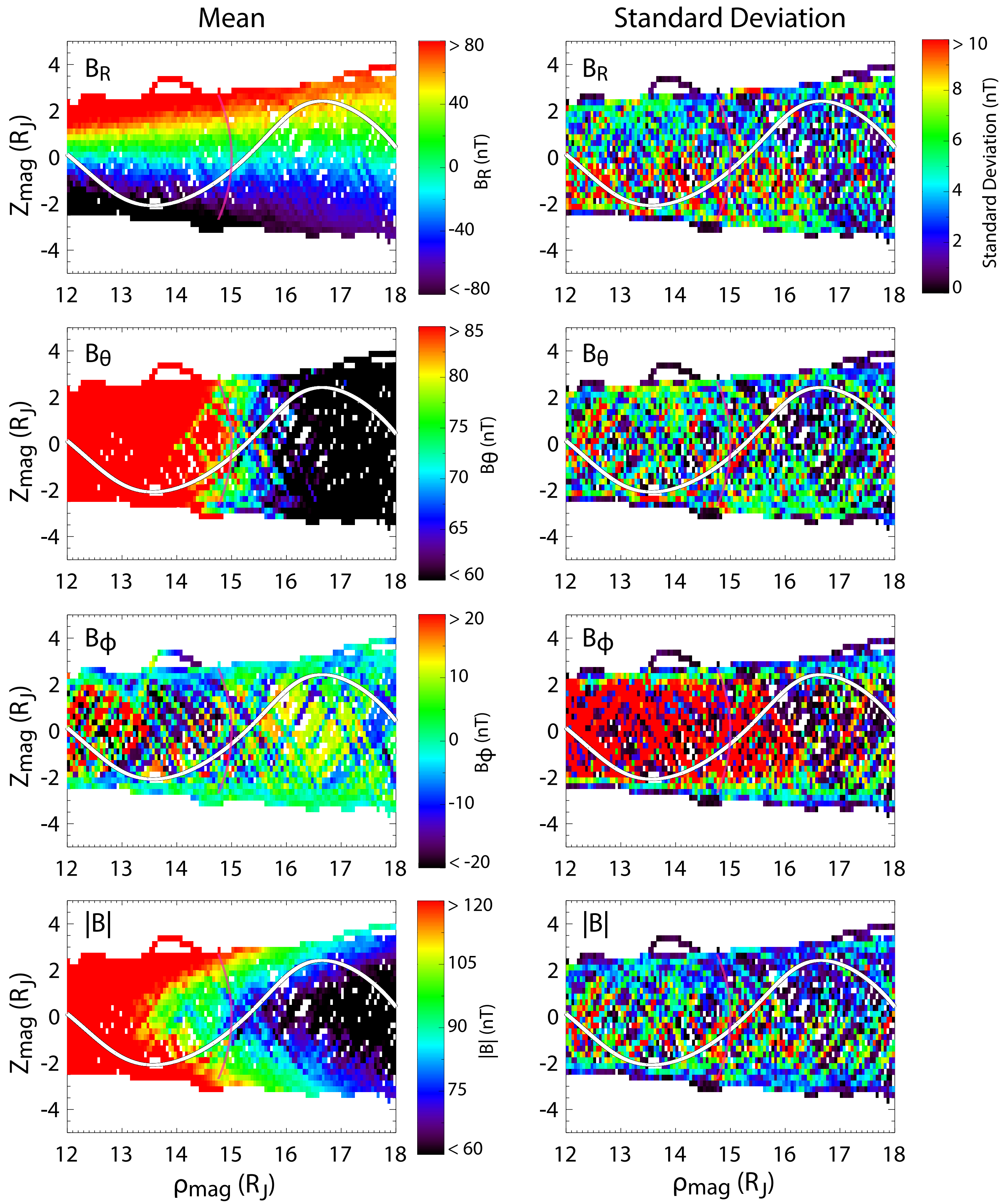

Mean
Standard Deviation
B_R
B_θ
B_ϕ
|B|
Z_{mag} (R_J)
ρ_{mag} (R_J)
B_R (nT)
$B\theta$ (nT)
$B\phi$ (nT)
|B| (nT)
Standard Deviation (nT)
> 80
< -80
> 85
< 60
> 20
< -20
> 120
> 10

Figure 5.

Juno Measured Field, **Galileo Average**, and **JRM09+CON2020 model** along Juno's orbit

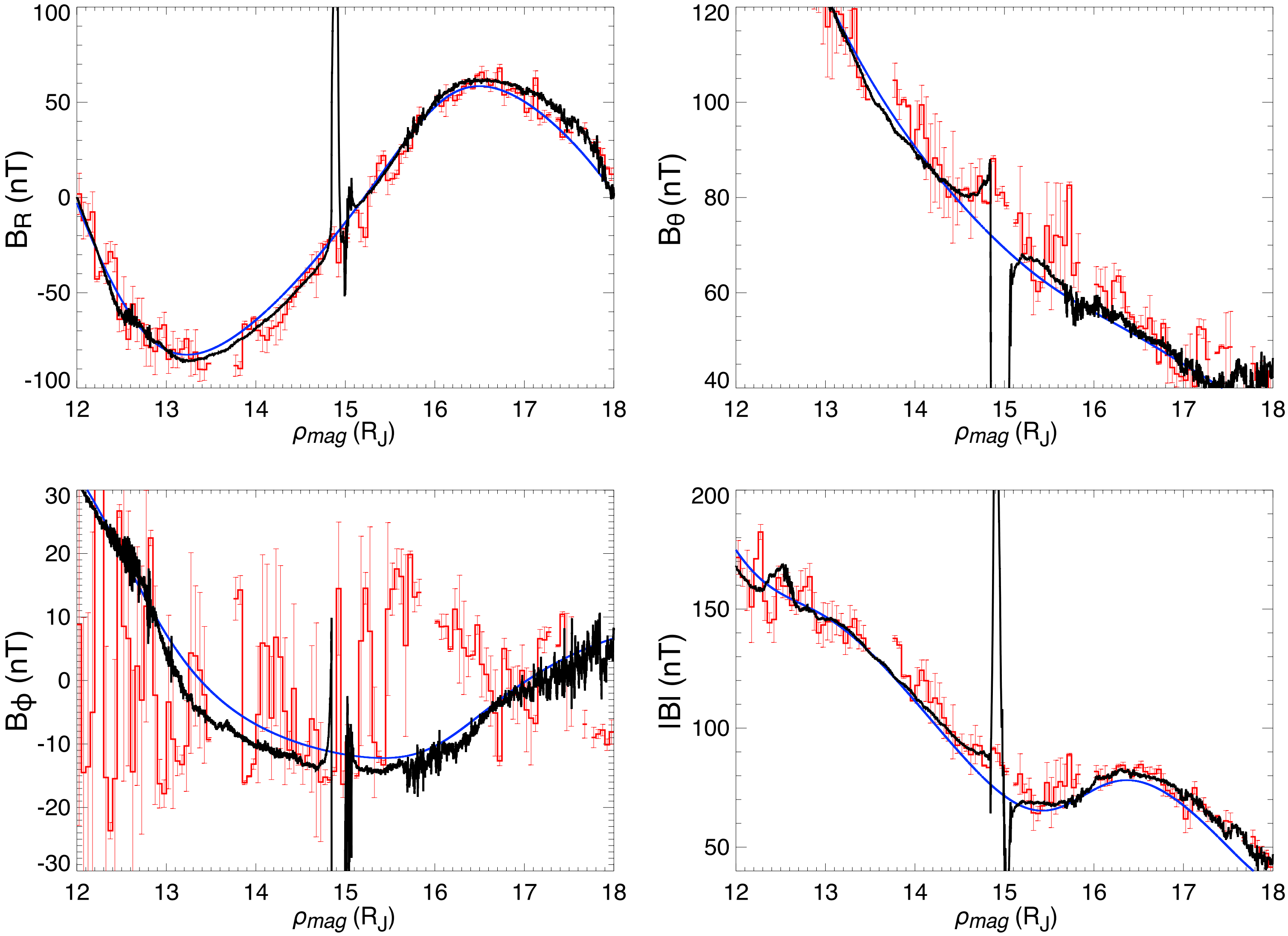

Figure A1.

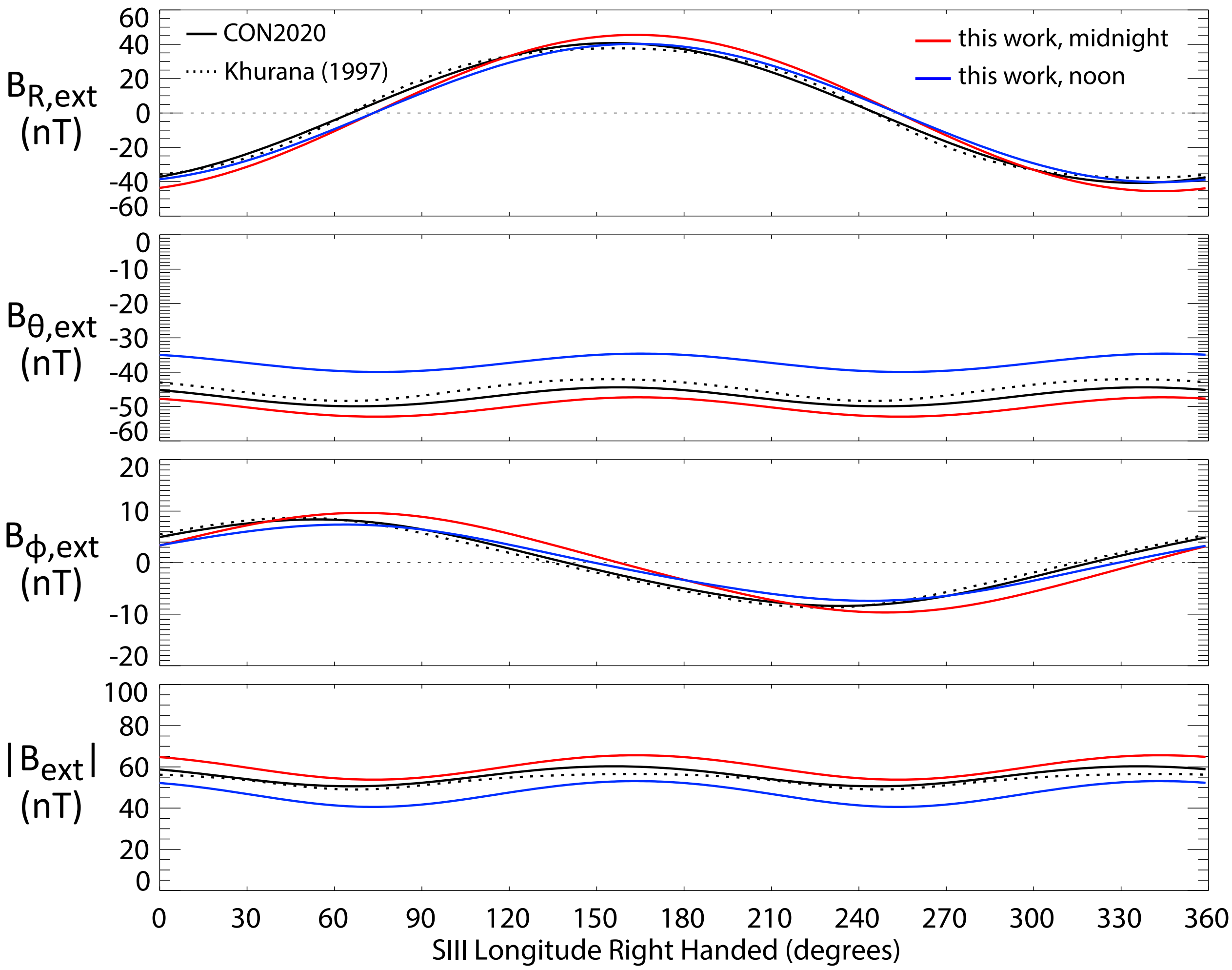

CON2020
Khurana (1997)
this work, midnight
this work, noon
B_R,ext (nT)
B_θ,ext (nT)
B_φ,ext (nT)
|B_ext| (nT)
SIII Longitude Right Handed (degrees)